AN EXPERIMENTAL STUDY ON APPLICATION OF HYBRID-TYPE BASE ISOLATION SYSTEM TO HIGH-RISE BUILDINGS

Ryota MASEKI[1], Ichiro NAGASHIMA[2] And Masayoshi HISANO[3]

SUMMARY

The performance of the hybrid-type base isolation system, which is composed of sliding bearings and laminated rubber bearings, is studied in this paper, in application to high-rise buildings with slender configurations. This base isolation system enables one to make the resonance period of base-isolated buildings comparatively long, up to 4 or 5 seconds. The shaking table tests were performed using a scaled 5-story frame model scaled to 1/17 of the prototype high-rise building, which is 65 meters high and has an aspect ratio of 5. Several major earthquake records were scaled to different peak ground velocities ranging from 25cm/s up to 100cm/s and used as input base excitations. Through the series of the tests, it was clarified that the stability of the frame model against overturning moment and the satisfactory base isolation effects were maintained even at the largest input excitation of 100 cm/s, at which the uplift of sliding bearings occurs and the tensile force is generated in laminated rubber bearings. To investigate the accuracy of the newly developed 3D-FEM analyses program that can consider the uplift and the fluctuating axial load of the bearings, the simulation analyses of the frame model were also conducted. It was shown that the response of the frame model, including the uplift of the sliding bearings and the tensile force of laminated rubber bearings, were well simulated with enough accuracy.

INTRODUCTION

The hybrid-type base isolation system, in which sliding bearings and laminated rubber bearings are combined, can make the resonance period of base-isolated buildings comparatively long up to 4 or 5 seconds, because the natural period of isolation buildings are determined only by the stiffness of the laminated rubber bearings when sliding bearings slide during earthquakes. Thus, this system can be applied to high-rise buildings and slender buildings to which the ordinary base isolation systems utilizing laminated rubber bearings alone, that make the resonance period of base-isolated buildings only up to about 3 seconds, are not applicable. In applying the base isolation system to these buildings, it is very important to clarify the stability of the system against the overturning moment and the isolation performance under severe ground excitations that may cause the uplift and the resulting tensile force in the isolation devices.

In this research, tri-axial shaking table tests were performed using a scaled building model to investigate the advantage of the hybrid-type base isolation system. The simulation analyses of the experimental results were also conducted to investigate the accuracy of the 3D-FEM analysis that can consider the fluctuating axial load of the bearings.

[1] *Taisei research institute, Taisei CORPORATION, Yokohama, Japan ryota.maseki@sakura.taisei.co.jp*
[2] *Taisei research institute, Taisei CORPORATION, Yokohama, Japan ichiro.nagashima@sakura.taisei.co.jp*
[3] *Seismic technology promotion department, Taisei CORPORATION, Shinjyuku, Japan masayoshi.hisano@sakura.taisei.co.jp*

EXPERIMENTAL MODEL

Figure 1. and Figure 2. show the frame model and the isolation bearings, respectively. Photo 1. shows the configuration of the frame model on the shaking table. Table 1. shows the law of similarity for this model. The prototype building of the model has the plan of 12 meters wide by 36 meters long, and the aspect ratio, which is defined as the ratio of the height to the width of the transverse direction, is five. The size of the frame model is scaled to 1/17, which is determined so that the acceleration and the vertical pressure of the bearings are equal to those of the prototype building. The superstructure of the frame model has one span in transverse direction and three spans in longitudinal direction (the plan of 75cm wide by 225cm long), and it has 5-story steel frame, with the height of 375cm. The total mass of the frame model is 1.5 x 10^4kg. The laminated rubber bearings are installed under the four middle columns and the elastic sliding bearings are installed under the four corner columns. The elastic sliding bearing has the thin poly-tetra-fluoro-ethylene (PTFE) plate on the chloroprene rubber layer of 1mm thickness whose diameter is 48mm, and it is supported on the stainless steel bearing plate. The laminated rubber bearing has the diameter 52mm, 8 layers of the natural rubber of 1mm thickness whose shear modulus G is 4.5kgf/cm^2. (1kgf/cm^2=98.0665kPa) The ratio of the axial load supported by the laminated rubber bearings is 55% of the total axial load, and the vertical pressures of all bearings are about 100kgf/cm^2.
The natural period of the frame model with base fixed condition is 0.32 seconds in transverse direction (1.3 seconds for the prototype building), and the natural periods of the base isolation model before and after sliding are 0.44 seconds and 1.14 seconds, respectively (1.8 seconds and 4.7 seconds, respectively for the prototype building), as listed in Table 2. and Table 3.

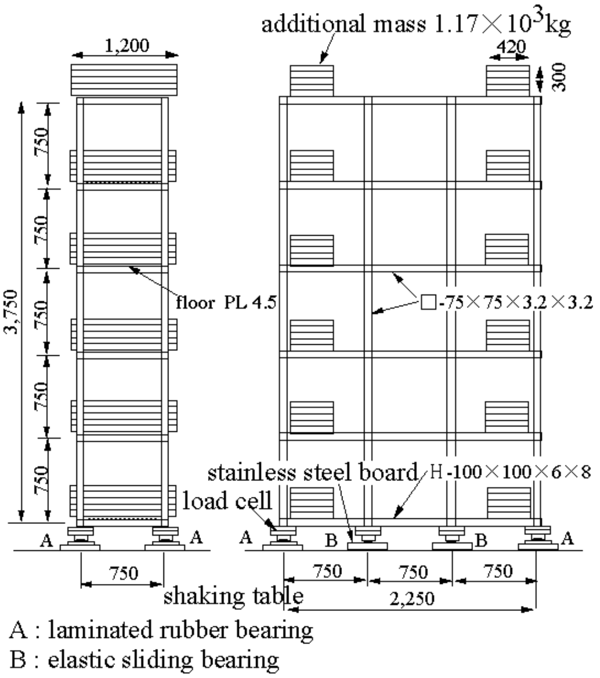

Figure1. Frame model of hybrid-type base isolation building.

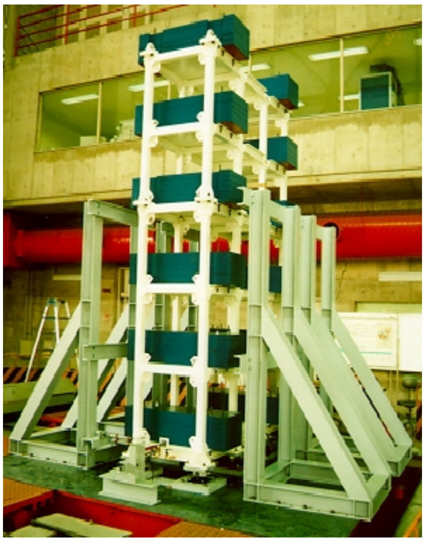

Photo1. Configuration of frame model.

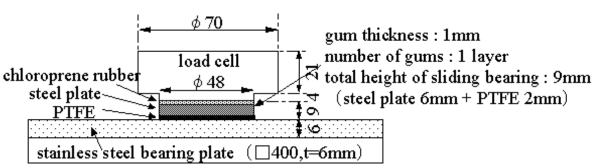

(a) elastic sliding bearing.

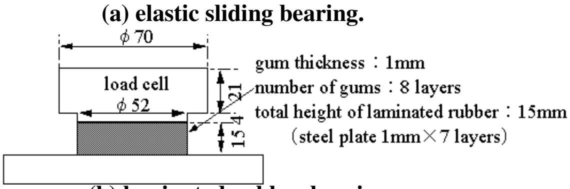

(b) laminated rubber bearing.

Figure2. Detail of isolation bearings.

Table1. Law of similarity.

		ratio			ratio
length	λ_L	1/17	displacement	λ_L	1/17
force (mass)	λ_P	1/289	velocity	λ_L/λ_T	$1/\sqrt{17}$
time (period)	λ_T	$1/\sqrt{17}$	acceleration	λ_L/λ_T^2	1.0
			vertical pressure	λ_P/λ_L^2	1.0

Table2. Frequency property of superstructure.

mode	direction	natural period (prototype building)	damping factor
1st	transverse	0.32sec (1.30sec)	0.016
2nd	longtudinal	0.26sec (1.08sec)	0.013

Table3. Frequency property of isolation model (before sliding).

mode	direction	natural period (prototype building)	damping factor
1st	transverse	0.44sec (1.83sec)	0.041
2nd	longtudinal	0.40sec (1.63sec)	0.051
3rd	transverse	0.14sec (0.59sec)	0.064
4th	longtudinal	0.12sec (0.51sec)	0.051

1kgf = 9.80665 N

To study the effects and the stability of the base isolation system, the records of El Centro (1940 El Centro earthquake), Hachinohe Harbor (1968 Hachinohe earthquake) and JMA Kobe (1995 Hyogoken-Nanbu earthquake) were used in the tri-axial shaking table tests. The larger component of the recorded horizontal ground motions was applied to the transverse direction of the frame model, and the peak ground velocity (PGV) of the ground excitation was increased gradually from $50cm/s^2$ up to 25cm/s, 50cm/s and 75cm/s for the prototype building. Furthermore, PGV of the JMA Kobe excitation was increased up to 100cm/s, to investigate the limit performance. And the total duration of earthquake records were reduced to $1/\sqrt{17}$ of the original records according to the law of similarity. As for the measurement, the horizontal and vertical acceleration on each story and the relative deformation of the isolation story were measured. And the fluctuating axial loads of the isolation bearings were also measured with the load cells.

EXPERIMENTAL RESULTS

Figure 3. shows (a)the maximum response acceleration of the top story, (b)the shearing coefficient of the first story, and (c)the maximum deformation of the isolation story. Figure 4(a) shows the maximum acceleration distributions at PGV of 50cm/s, and Figure 4(b) shows the maximum acceleration distributions at 50cm/s, 75cm/s and 100cm/s under the JMA Kobe excitation. Table 4. indicates the occurrence of the uplift of the sliding bearings and the tensile stress in the laminated rubber bearings. Figure 5. shows the response acceleration of the top story, the relative displacement of the isolation story, and the fluctuating axial load acting on the elastic sliding bearings and the laminated rubber bearings at PGV of 100cm/s under the JMA Kobe excitation.

When the input acceleration is below 50 cm/s^2 or so, sliding does not occur in the sliding bearings and the isolation effects are limited; the ratio of the maximum response acceleration to the input ground acceleration (acceleration reduction ratio) is about 1.2. As the input acceleration increases, sliding occurs in the sliding bearings and the isolation effects can be obtained; the acceleration reduction ratio becomes 0.88 – 1.1 at PGV of 25cm/s, 0.62- 0.76 at PGV of 50 cm/s, and 0.59 – 0.62 at PGV of 75 cm/s. As is seen in Figure 4(a), the distributions of the maximum acceleration become smallest in the middle story, which indicates that the secondary mode of vibration dominates in the slender high-rise buildings with the base isolation system.
The shearing force coefficient of the first story is less than 0.15 at PGV of 50cm/s and is kept under 0.17 even at PGV of 75cm/s. The maximum horizontal deformation of the isolation floor is 1.51cm (26cm for the prototype building) at PGV of 100cm/s under the JMA Kobe excitation and is smaller than the allowable design deformation of 1.76cm (30cm for the prototype building).

The occurrence of the uplift and the tensile stress in the laminated rubber bearing is observed several times in Figure 5. Because the uplift occurs more frequently, the distribution of the maximum acceleration is slightly different at PGV of 100cm/s in comparison with the cases at PGV 50cm/s and 75cm/s under the JMA Kobe excitation as is seen Figure 4(b). However, the acceleration reduction ratio of 0.5 – 0.7 is attained and large pulse due to the uplift and the tensile stress isn't seen in the horizontal and vertical acceleration of the frame model and the deformation of the isolation story. The stability of the test frame against severe earthquake is thereby clarified.

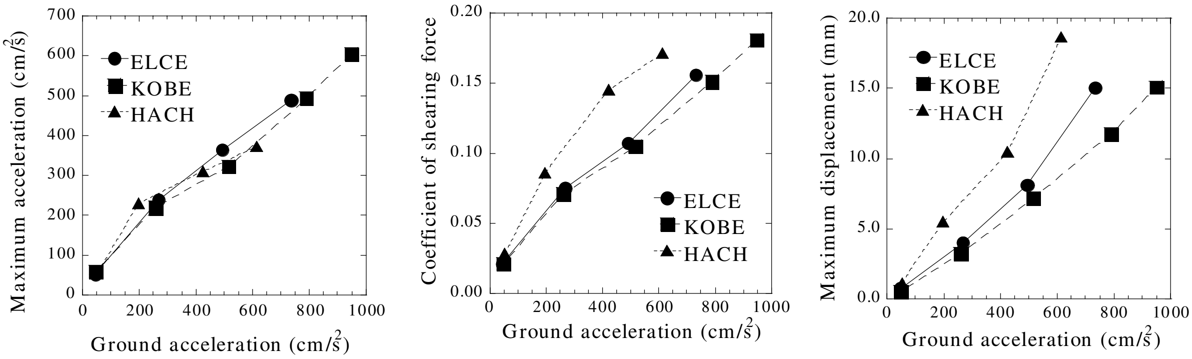

(a) Acceleration of top story. **(b) Shearing coef. of the 1st story.** **(c) Displacement of isolation story.**

Figure 3. Maximum response of frame model.

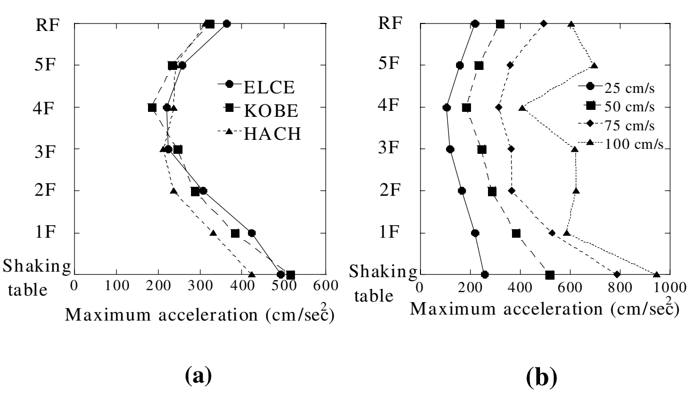

Figure4. Distribution of maximum acceleration: (a) at PGV of 50cm/s; (b) in case of JMA Kobe

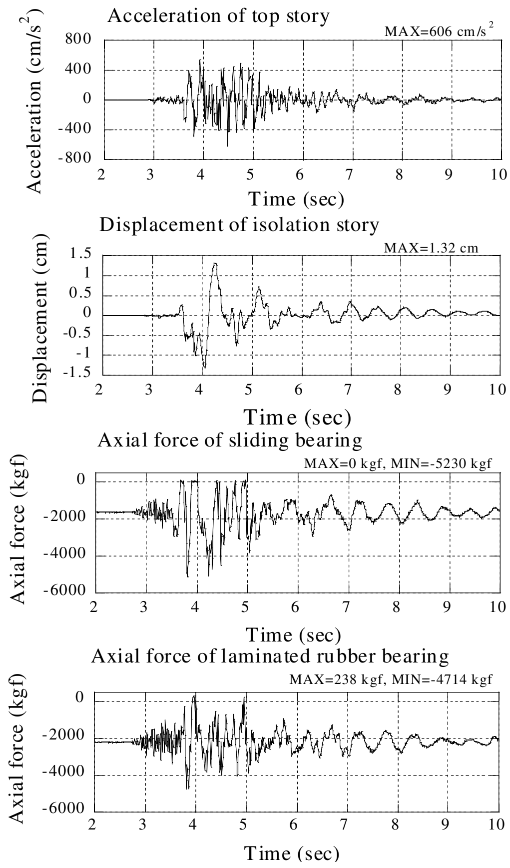

Figure5. Response of frame model under the excitation of JMA Kobe 100cm/s.

Table4. Occurrence of uplift and tensile stress.

		25 cm/s	50 cm/s	75 cm/s	100 cm/s
EL CENTRO	uplift	×	#	#	
	tensile stress	×	×	#	
JMA KOBE	uplift	×	#	#	#
	tensile stress	×	×	#	#
HACHINOHE HARBOR	uplift	×	#	#	
	tensile stress	×	#	#	

\# means occurrence

NUMERICAL MODEL

The numerical model is depicted in Figure 6.The superstructure is constructed with the 3D beam elements. The elastic sliding bearing is composed of the horizontal shear springs and the vertical spring; the horizontal springs are modelled by a 'multi-spring element' that realizes the same force – deformation relationships in all horizontal directions. When the shear force in the horizontal spring reaches the friction force, sliding occurs and the force that is transmitted to the superstructure is limited to the friction force. The coefficient of friction for the sliding bearings is assumed as 0.1 based on the measured shear force – deformation relationships of the isolation story.

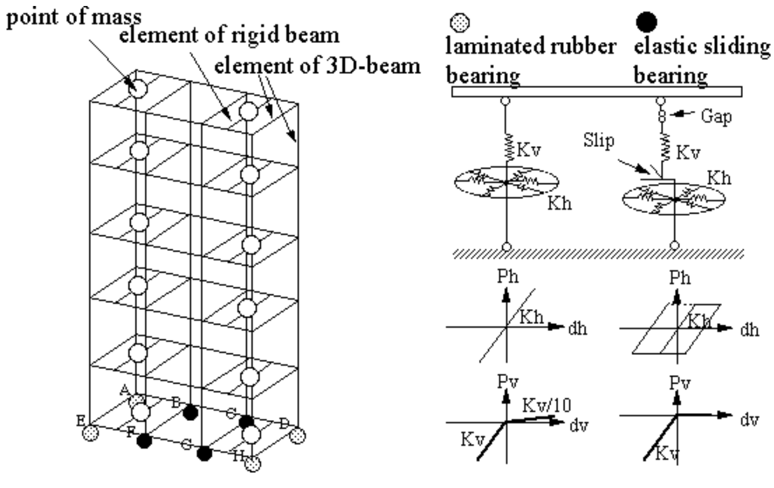

Figure 6. 3D-FEM model.

The vertical spring of the elastic sliding bearing is modelled by a ‘gap element’ such that the vertical stress becomes zero when the uplift occurs. The vertical spring of the laminated rubber bearing is modelled by a ‘non-linear elastic spring element’ such that the spring constant in the tensile side is 1/10 of that in the compression side. As for the inherent structural damping, it is assumed that the damping matrix is proportional to the stiffness matrix for the higher modes, over 5th, and, in addition to that, the modal damping factors are assigned for the lower modes up to the 4th modes as shown in Table 3.

RESULTS OF SIMULATION

As an example of the 3D-FEM analyses, the responses of the frame model subjected to the excitation of Hachinohe earthquakes with different PGV are presented.

Figure 7. shows the responses of the frame model subjected to the excitation of Hachinohe earthquake with PGV of 50cm/s; the acceleration, the deformation of the isolation story, the fluctuating axial load on the sliding bearing B as well as the laminated rubber bearing A, illustrated in Figure 6., and the horizontal deformation locus of the isolation story are measured and compared with the corresponding simulated responses. The fluctuating axial load on the sliding bearing B and on the laminated rubber bearing A are shown in Figure 7(d) and (e), respectively. The zero axial force in Figure 7(d) indicates the occurrence of the uplift of the sliding bearing; the uplift of the sliding bearings observed around 4.5 second are accurately simulated. The negative and the positive signs in Figure 7(e) show the compression and tensile stress, respectively. As is observed in the shearing force - shear deformation relationship of the isolation story shown in Figure 7(f), the effects of the fluctuating axial load on the friction force are measured and properly simulated. Table 5. shows the comparison of the maximum response in the experiment and the simulation.

Through the comparisons mentioned above, it is shown that the measured responses are simulated by the 3D-FEM analyses with reasonable accuracy.

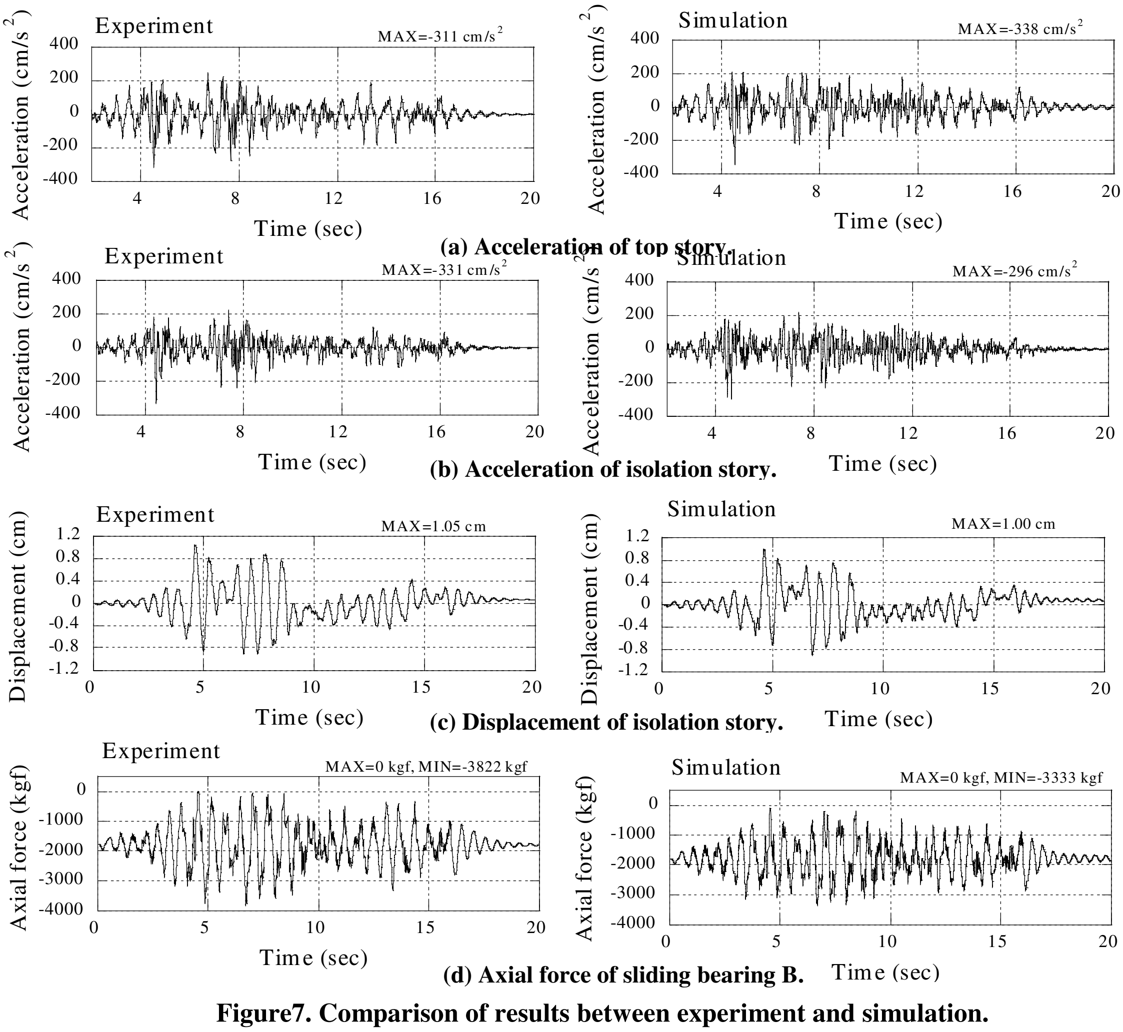

(a) Acceleration of top story.

(b) Acceleration of isolation story.

(c) Displacement of isolation story.

(d) Axial force of sliding bearing B.

Figure7. Comparison of results between experiment and simulation.

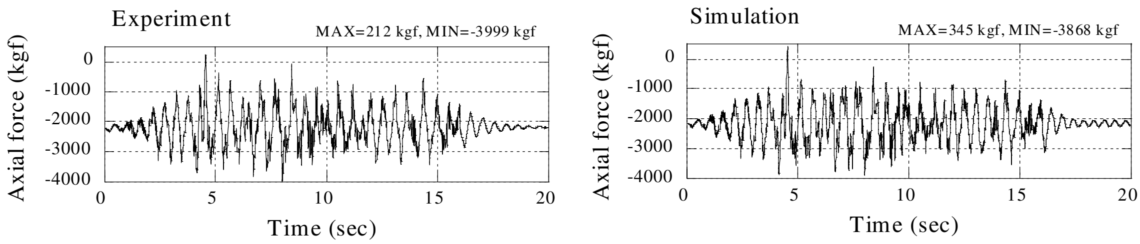

(e) Axial force of laminated rubber bearing A.

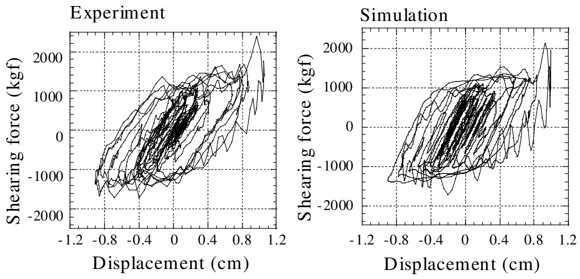

(f) Shear force-displacement curve of isolation story.

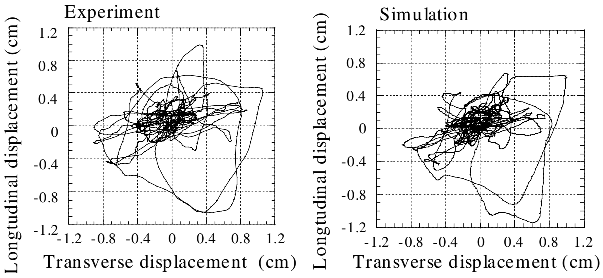

(g) Horizontal deformation locus of isolation story .

Figure7. Comparison of results between experiment and simulation.

Table 5. Comparison of maximum response between experiment and simulation.

HACHINOHE		25cm/s		50cm/s		75cm/s	
		EXP	SIM	EXP	SIM	EXP	SIM
Acceleration of top story (cm/s^2)		230	189	311	338	372	404
Displacement of isolation story (cm)		0.6	0.4	1.1	1.0	1.9	1.8
Axial force in sliding bearing (kgf)	MIN	-3316	-2707	-3822	-3333	-4270	-3766
	MAX	-253	-457	0 (*)	0 (*)	0 (*)	0 (*)
Axial force in laminated rubber bearing (kgf)	MIN	-3313	-3043	-3999	-3868	-4349	-4108
	MAX	-658	-911	212 (#)	345 (#)	390 (#)	493 (#)
tensile stress in laminated rubber bearing (kgf/cm^2)				10.0	16.2	18.3	23.2

negative and positive signs in axial force show the compression and tesile stress, respectively
(*) and (#) mean the occurrence of uplift and tensile stress, respectively

CONCLUSIONS

The shaking table tests and the analyses led to the following conclusions:

1) As the input excitation becomes very strong, uplift and resulting tensile stress in isolation devices occur. But the behavior of the building is stable and the uplift of the sliding bearings has little influence on horizontal response of the building. Even under the severest excitation of the JMA Kobe, scaled to PGV of 100cm/s, the frame model remains stable and maintains satisfactory isolation effects.

2) The response of the frame model, involving the fluctuating axial force of isolation devices, can be accurately simulated through the 3D sliding analysis technique. Also the uplift of the sliding bearings and the tensile force of laminated rubber bearings can be simulated with reasonable accuracy.